Steep Anomalous Dispersion in Coherently Prepared Rb Vapor

A. M. Akulshin,[1,2] S. Barreiro,[1] and A. Lezama[1]
[1]*Instituto de Física, Facultad de Ingeniería, C. Postal.30. 11000, Montevideo, Uruguay*
[2]*P. N. Lebedev Physics Institute, 117924 Moscow, Russia*
(Received 4 June 1999)

Steep dispersion of opposite signs in driven degenerate two-level atomic transitions have been predicted and observed on the D_2 line of ^{87}Rb in an optically thin vapor cell. The intensity dependence of the anomalous dispersion has been studied. The maximum observed value of anomalous dispersion ($dn/d\nu \simeq -6 \times 10^{-11}$ Hz^{-1}) corresponds to a negative group velocity $V_g \simeq -c/23\,000$.

PACS numbers: 42.50.Gy, 32.80.Qk, 42.62.Fi

Investigations of coherent effects in resonant media, namely coherent population trapping (CPT) and electromagnetically induced transparency (EIT) [1,2], which can dramatically modify the absorptive and dispersive properties of an atomic vapor, have caused a rebirth of interest in the problem of light propagation through a dispersive medium. In the last decade, the study of the dispersive properties of coherently prepared media was always under attention due to fundamental and practical interest.

An ultralarge index of refraction in coherently prepared resonant gas was predicted [3], and a refractive index variation as large as $\Delta n \approx 1 \times 10^{-4}$ was demonstrated in a dense Rb vapor [4]. It was also shown that a coherently driven medium exhibits large dispersion [5]. A high normal dispersion (up to $dn/d\nu \simeq 1 \times 10^{-11}$ Hz^{-1}) was measured on the Cs D_2 line in a vapor cell [6] and in an atomic beam [7]. Extremely slow light group velocity (17 m/s) associated with normal dispersion was demonstrated in an ultracold atomic sample [8]. However, recent experiments show that the same order of magnitude of group velocity can be observed using heated [9] and room temperature [10] vapor cells.

All these investigations were carried out on alkaline atoms where the absorption is strongly suppressed and dispersion is steep and normal ($D \equiv dn/d\nu > 0$) due to CPT between the two ground-state hyperfine levels (Λ scheme). However, atomic coherence among Zeeman sublevels belonging to the same ground-state hyperfine level can lead not only to usual EIT, but also to an absorption enhancement named as *electromagnetically induced absorption* (EIA) [11,12]. Since EIT/EIA effects in degenerate two-level systems can produce a significant variation in the absorption with subnatural width, one can predict a large absolute value of dispersion in this case. Notice that at resonance, dispersion would be normal ($D > 0$) for EIT and anomalous ($D < 0$) for EIA. In both cases, the absolute value of the dispersion can be several orders of magnitude greater than for a linear medium. This Letter presents the observation of steep anomalous and normal dispersion in a coherently prepared degenerate two-level atomic system.

Refractive index and dispersion were analyzed with the model recently used to study subnatural EIA resonances [13]. In this model, two monochromatic optical fields, a drive field and a weak probe field with amplitudes E_d, E_p and frequencies ω_d, ω_p, respectively, are incident on motionless two-level atoms with resonance frequency ω_0 and electric dipole moment μ. The atomic levels are degenerate. The configuration is closed. The spontaneous decay rate is Γ. The return of the system to thermal equilibrium is described by a relaxation rate γ ($\gamma \ll \Gamma$) determined in our case by the finite time-of-flight of the atoms through the interaction zone. The drive wave Rabi frequency is $\Omega = \mu E_d/\hbar$ and its saturation parameter $S \equiv 2\Omega^2/\Gamma^2$.

The calculated refractive index, tested by the probe wave in the presence of the drive field, as a function of the frequency offset $\delta \equiv \omega_d - \omega_p$ is presented in the inset of Fig. 1. The shown spectra correspond to the closed transitions in the D_2 line of ^{87}Rb. The peak-to-peak refractive index variation Δn is higher for the anomalous dispersion because the transition $F_g = 2 \rightarrow F_e = 3$ is stronger than

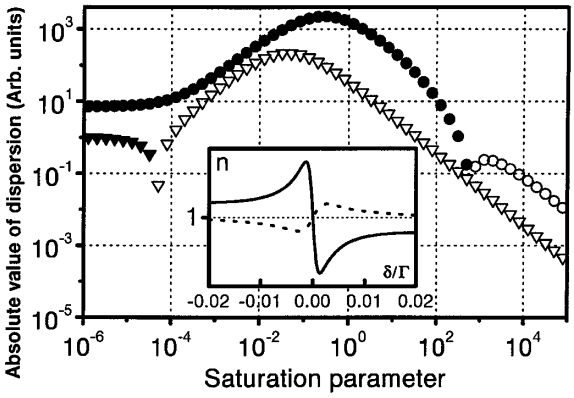

FIG. 1. Calculated dispersion at $\delta = 0$ for the transitions $F_g = 2 \rightarrow F_e = 3$ (circles) and $F_g = 1 \rightarrow F_e = 0$ (triangles) as a function of the saturation parameter S. Solid (hollow) points correspond to negative (positive) dispersion. Inset: Calculated refractive index as a function of δ for linear and orthogonal pump and probe polarizations for these transitions and same drive field intensity ($\omega_d = \omega_0$, $\Gamma/\gamma = 1000$, $S \lesssim 1$).

the $F_g = 1 \rightarrow F_e = 0$ transition. The corresponding absolute value of the anomalous dispersion is also larger.

The values of D and n depend on light intensity, atomic density N, level degeneracy, and polarizations, among other parameters. Here we restrict our attention to the dependence with the drive-field intensity I_d.

Since a general expression for n in driven degenerate two-level systems is not available at present, we consider as a guide the analytical expression corresponding to the ideal Λ scheme [7]:

$$n(\delta) = 1 + \frac{3}{8\pi^2}\lambda^3 N \frac{\Omega^2\delta}{(\Omega^2 + \Gamma\gamma/2)^2 + (\gamma\delta/2)^2}, \quad (1)$$

where λ is the wavelength of the optical transition. At low intensity ($\Omega^2 \ll \Gamma\gamma$) Δn and D around $\delta = 0$ are growing linearly with Ω^2. For high intensity ($\Omega^2 \gg \Gamma\gamma$), D and Δn are inversely proportional to Ω^2. It can be shown that the maximum for Δn and D are reached for $\Omega^2 = \Gamma\gamma/2$ when the saturation parameter $S = \gamma/\Gamma$.

Such behavior may be explained in the following way: At low intensity, when power broadening is not significant (the width of the resonance is determined by the ground-state relaxation), the amplitude is growing linearly with intensity, while the width remains almost constant. In this case, D grows linearly with I_d. The dispersion saturates when the resonance width is determined by power broadening. At high intensity, the refractive index and the absorption saturate [13], while the resonance width still grows. So, in this region D decreases with intensity.

The calculated intensity dependences of the dispersion at resonance ($\delta = 0$) shown in Fig. 1 are in qualitative agreement with the simple analytical expression [Eq. (1)] for low and high drive intensity. At very low drive intensity (linear absorption) the dispersion for the two transitions considered in Fig. 1 is anomalous. For higher drive intensity there is absorption enhancement (EIA) for one transition and absorption reduction (EIT) for the other. The first case results in anomalous dispersion, while the second one corresponds to normal dispersion. The two curves have a maximum at moderate intensity ($S \lesssim 1$). At large drive intensities ($S > 10^3$) the dispersion on both transitions is normal and exhibits the same linear asymptotic behavior.

The experiment was realized on the D_2 line of ^{87}Rb in a vapor cell. We used a phase heterodyne method to measure the refractive index. The idea of this approach is based on the well-known method of FM spectroscopy and the two-mode technique [14]. Our method is similar to that used for dispersion measurements [7] and for Doppler-free spectroscopy [15]. To obtain information about n, the phase of a rf signal produced by mixing the resonant probe wave with a nonresonant auxiliary wave (having the same optical path) is compared to an rf reference produced by the mixing of undisturbed fractions of the probe and the auxiliary waves. The variation of the phase difference between the two rf signals, due to the atomic medium dispersion, is $\delta\Phi = l(n - 1)\omega/c$, where l is the vapor cell length. With these techniques, the influence of acoustic noise is dramatically reduced compared to the homodyne method based on a Mach-Zehnder interferometer [4,6].

The scheme of the experimental setup is shown in Fig. 2. A single-mode extended cavity diode laser frequency lockable to a Rb saturated absorption resonance was used. Two mutually coherent waves with tunable optical frequency offset were obtained by using two acousto-optic modulators (AOM's 1,2) [11]. The diffracted output from AOM2, driven by a tunable rf generator, was used as the drive wave. The two outputs of AOM3 (with fixed frequency offset) were combined on the beam splitter BS1. One of the beam splitter outputs was used as the signal wave. It contains two frequency components, the resonant probe wave, with variable detuning δ ($\delta \ll \Gamma$) with respect to the drive field and the auxiliary wave (80 MHz apart). Notice that under these conditions the auxiliary wave does not interact with the same atomic velocity class as the drive and probe fields. The second output of BS1 was used to produce the rf reference on the photodiode (PD1). Signal and drive waves with orthogonal linear polarizations were superimposed on the polarization beam splitter BS2. After spatial filtering in a 50-cm-long single-mode optical fiber, the pump and signal waves were sent through a 5-cm-long Rb cell at room temperature. The external magnetic field at the cell was reduced to a 10 mG level using a μ-metal shield. Maximum powers of the drive and the signal waves at the cell were 0.15 and 0.04 mW, respectively. A double balanced mixer (DBM) was used as a phase detector. The voltage-to-phase response of the DBM was calibrated introducing known delays between the two inputs. A lock-in amplifier was used for signal processing while the drive wave was chopped ($\sim$1 kHz).

Experimental spectra of the probe wave phase variation on transitions from the two ground-state hyperfine levels (at the same conditions) are shown in Fig. 3a. Around $\delta = 0$ the phase variations have opposite slope signs corresponding to opposite signs of the dispersion. The line

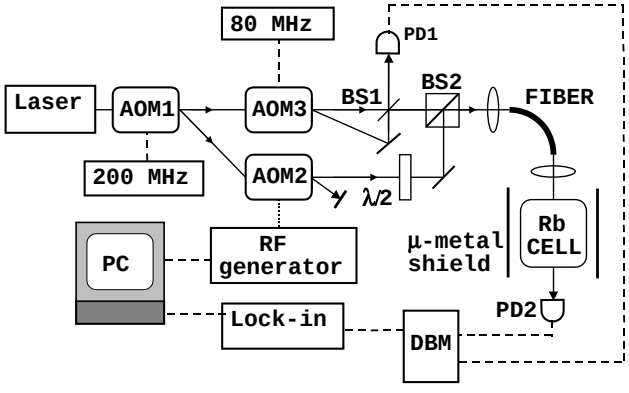

FIG. 2. Experimental setup.

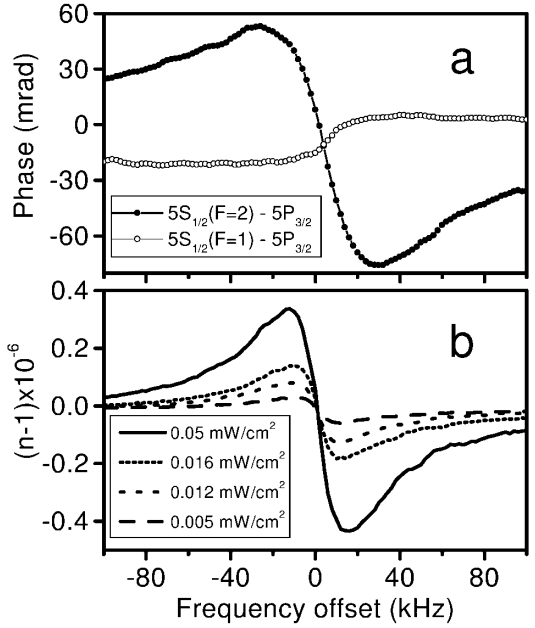

FIG. 3. (a) Phase resonances for laser frequencies corresponding to the transitions $5S_{1/2}(F_g = 2) - 5P_{3/2}(F_e = 3)$ and $5S_{1/2}(F_g = 1) - 5P_{3/2}(F_e = 0)$ of ^{87}Rb (beam diameter: 0.8 cm, drive intensity: 0.3 mW/cm^2). (b) Refractive index for the transition $5S_{1/2}(F_g = 2) - 5P_{3/2}(F_e = 3)$ as a function of δ for different values of I_d and beam diameter 1.6 cm.

shapes are in reasonable agreement with the spectra calculated for motionless atoms and single closed transitions (Fig. 1). This agreement may seem rather surprising since in the experiment, due to the velocity distribution, three different atomic transitions, one closed and two open, contribute to the signal in each case. On all open transitions as well as on the closed $F_g = 1 \rightarrow F_e = 0$ transition, EIT occurs and, consequently, the dispersion is normal—only on the $F_g = 2 \rightarrow F_e = 3$ transition EIA takes place and the dispersion is anomalous [13]. However, due to optical pumping the signal is essentially determined by the closed transitions resulting in the qualitative agreement with the theoretical prediction. To compare quantitatively the experimental spectra with theory, velocity distribution, excited state hyperfine splitting and optical depopulation of open transitions should be taken into account.

The value of $\Delta n = c\delta\Phi/\omega l$ can be obtained taking into account the cell length ($l = 5$ cm). The error in the measured absolute value of the refractive index and the dispersion was around 15%. However, the reproducibility of relative measurements was within 2%.

In the following, we investigate the intensity dependence of the steep anomalous dispersion [6]. Experimental spectra of the refractive index for different values of the drive intensity are shown in Fig. 3b. I_d was varied from 0.005 to 0.05 mW/cm^2 by using filters while the light diameter in the cell was 1.6 cm. At such low intensities Δn and D are growing linearly with intensity. In this case, the refractive index can be characterized by a nonlinear Kerr coefficient n_2: $[n = n_1 + n_2 I_d]$. Notice that the value of n_2 is a rapidly varying function of δ. At $\delta = 16$ kHz we have $n_2 \simeq 8 \times 10^{-3}$ cm^2/W. The maximum observed dispersion at low drive intensity was $D_{\max} \simeq -6 \times 10^{-11}$ Hz^{-1}.

Based on the previous considerations, the attempt was made to maximize the dispersion by increasing the drive intensity. Because of laser power limitation, the increase of I_d was obtained through light cross-section reduction using a telescope. For three different diameters (1.6, 1.0, and 0.6 cm), the drive wave attenuation resulted in dispersion reduction (Fig. 4) indicating that we were in the region below the maximum of the dependence $D(I_d)$. The absolute values of D and n_2 were reduced ($n_2 \simeq 2 \times 10^{-3}$ cm^2/W and $n_2 \approx 5 \times 10^{-4}$ cm^2/W for 1.0 cm and 0.6 cm drive beam diameter, respectively) in spite of the fact that the intensity was higher. However, we should notice that the light cross-section reduction results in a shortening of the interaction time (associated to γ in our model) which participates in the atomic dynamics and determines the minimum resonance width. The observed reduction of the dispersion for smaller beam diameters indicates that the role of the interaction time is essential—only at light wave diameter close to 0.4 cm we were able to reach a maximum in the $D(I_d)$ dependence. At relatively high intensity ($I_d > 1$ mW/cm^2) the dispersion decreases with drive intensity, and the refractive index profile becomes significantly different from a dispersion function (see inset of Fig. 4). We noticed that within some range of intensity, D (around $\delta = 0$) is almost independent on I_d, while the spectral distance between extrema of $n(\delta)$ is growing with I_d. This distortion reflects the influence of different time constants. The precise comparison with theory requires a detailed consideration of the transient behavior of the coherent medium.

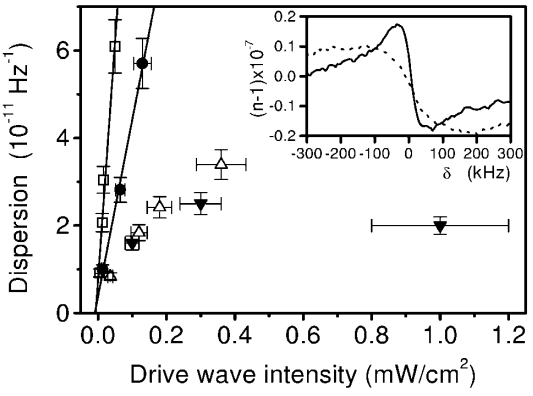

FIG. 4. Measured dispersion for different beam diameters ⌀. Squares: ⌀ = 1.6 cm; circles: ⌀ = 1.0 cm; hollow triangles: ⌀ = 0.6 cm; solid triangles: ⌀ = 0.4 cm. Solid lines are linear fits. The laser frequency was locked to the Doppler-free resonance on the $5S_{1/2}(F_g = 2) \rightarrow 5P_{3/2}(F_e = 3)$ transition. Inset: Refractive index as a function of δ for ⌀ = 0.3 cm and different intensities. Solid line: $I_d = 0.2$ mW/cm^2; dotted line: $I_d = 2$ mW/cm^2.

It is possible to characterize a dispersive medium by a light group velocity $V_g = c/(n + \nu \times dn/d\nu)$. Steep dispersion ($|dn/d\nu| \gg n/\nu$) is intimately associated with large modifications of the group velocity near the resonance. The maximum-obtained value of steep anomalous dispersion $D_{\max} \simeq -6 \times 10^{-11}$ Hz^{-1} corresponds to a rather slow negative group velocity $V_g \simeq -c/23\,000$. It is interesting to mention that for $dn/d\nu < 0$ the value of V_g can be infinitely large with opposite signs allowing for intriguing effects such as superluminality [16]. In our case, infinite V_g should occur at relatively low anomalous dispersion ($dn/d\nu \simeq -n/\nu \simeq -2.6 \times 10^{-15}$ Hz^{-1}). According to the linear fits on Fig. 4 this can be easily obtained with a very weak drive intensity $I_d \sim 10^{-5}$ mW/cm^2. Also in our case a wide range group-velocity variation can be achieved by switching between normal and anomalous dispersion (selecting the atomic transition) and/or varying the drive intensity.

Large dispersion is interesting for different applications. Several ways, in addition to optimizing I_d, can be considered to increase the dispersion (both normal and anomalous) in degenerate two-level systems. Since n and D are proportional to the atomic density while the resonant medium is thin, it is possible to obtain higher dispersion at higher N. In an optically thick medium, thanks to EIT, further increase of normal dispersion is possible [17]. Another possibility is to use a medium with very slow ground state relaxation, for instance in a cell with buffer gas [18] or a cell with an antirelaxation coating [19]. According to Eq. (1) one can expect that in this case less intensity is needed to reach the maximum of the $D(I_d)$ dependence ($\Omega^2_{\max} \sim \gamma\Gamma/2$).

Coherently prepared media with optically controlled dispersion can be of interest for the design of new devices for pulse delaying/compressing in communication systems and optical computing. Also, the use of steep magnetically dependent dispersion for high precision magnetometry was discussed in detail [20]. We should notice, however, that the requirements on the coherent medium are somehow different for these applications. For pulse processing elements the bandwidth should be rather wide to permit operation with short pulses. On the other hand, higher sensitivity for low frequency variations of magnetic field requires narrow resonances. Steep dispersion on driven degenerate two-level systems appears suitable for the two types of applications.

In conclusion, we have demonstrated for the first time, in agreement with the theoretical prediction, steep normal and anomalous dispersion in a driven degenerate two-level atomic system. This result clearly stresses the importance of degenerate two-level systems for the investigation of quantum coherence and applications.

This work was supported by CONICYT (Project No. 92048), CSIC, and PEDECIBA (Uruguayan agencies).

[1] S. E. Harris, Phys. Today **50**, No. 7, 36 (1997).
[2] E. Arimondo, in *Progress in Optics XXXV*, edited by E. Wolf (Elsevier, Amsterdam, 1996), p. 257, and references therein.
[3] M. O. Scully, Phys. Rev. Lett. **67**, 1855 (1991).
[4] A. S. Zibrov *et al.*, Phys. Rev. Lett. **76**, 3935 (1996).
[5] S. E. Harris, J. E. Field, and A. Kasapi, Phys. Rev. A **46**, R29 (1992).
[6] O. Schmidt, R. Wynands, Z. Hussein, and D. Meschede, Phys. Rev. A **53**, R27 (1996).
[7] G. Müller, A. Wicht, R. Rinkleff, and K. Danzmann, Opt. Commun. **127**, 37 (1996).
[8] L. V. Hau, S. E. Harris, Z. Dutton, and C. H. Behroozi, Nature (London) **397**, 594 (1999).
[9] M. M. Kash, V. A. Sautenkov, A. S. Zibrov, L. Hollberg, G. R. Welch, M. D. Lukin, Yu. Rostovtsev, E. S. Fry, and M. Scully, Phys. Rev. Lett. **82**, 5229 (1999).
[10] D. Budker, D. F. Kimball, S. M. Rochester, and V. V. Yashchuk, Phys. Rev. Lett. **83**, 1767 (1999).
[11] A. M. Akulshin, S. Barreiro, and A. Lezama, Phys. Rev. A **57**, 2996 (1998); A. M. Akulshin, S. Barreiro, and A. Lezama, Proc. SPIE Int. Soc. Opt. Eng. **3485**, 194 (1998).
[12] A. V. Taichenachev, A. M. Tumaikin, and V. I. Yudin, JETP Lett. **69**, 819 (1999) [Pis'ma Zh. Eksp. Teor. Fiz. **69**, 776 (1999)].
[13] A. Lezama, S. Barreiro, and A. M. Akulshin, Phys. Rev. A **59**, 4732 (1999).
[14] N. G. Basov, M. A. Gubin, V. V. Nikitin, A. V. Nikulchin, D. A. Tyurikov, V. N. Petrovskiy, and E. D. Protsenko, J. Phys. (Paris) **42**, 89 (1981).
[15] D. Tyurikov, G. Kramer, and B. Lipphardt, IEEE Trans. Instrum. Meas. **46**, 174 (1997).
[16] See R. Y. Ciao and A. M. Steinberg, in *Progress in Optics XXXVII*, edited by E. Wolf (Elsevier, Amsterdam, 1997), p. 345, and references therein.
[17] M. D. Lukin *et al.*, Phys. Rev. Lett. **79**, 2959 (1997).
[18] S. Brandt, A. Nagel, R. Wynands, and D. Meschede, Phys. Rev. A **56**, R1063 (1997).
[19] D. Budker, V. Yashchuk, and M. Zolotorev, Phys. Rev. Lett. **81**, 5788 (1998).
[20] M. O. Scully and M. Fleischhauer, Phys. Rev. Lett. **69**, 1360 (1992); H. Lee, M. Fleischhauer, and M. Scully, Phys. Rev. A **58**, 2587 (1998), and references therein.